Copyright © 2003 American Scientific Publishers.
All rights reserved
Printed in the United States of America

SENSOR LETTERS
Vol. 1. 25–32, 2003

COMMUNICATION

Detection of Explosive Compounds with the Use of Microcantilevers with Nanoporous Coatings

P. G. Datskos,[a, b, *] N. V. Lavrik,[a] and M. J. Sepaniak[b]

[a]*Oak Ridge National Laboratory, Oak Ridge, Tennessee 37831-8039, USA*
[b]*University of Tennessee, Knoxville, Tennessee 37996-1200, USA*

(Received: 1 September 2003. Revised/Accepted: 10 September 2003)

Real-time detection of nitroaromatic explosive compounds in various environments is a challenging task for forensics, antiterrorist activities, and global de-mining projects. The ability to detect trace levels of trinitrotoluene (TNT) in air and soil is a key measure in reducing fatalities from land mines among civilians and tracking explosive materials. In the present work we demonstrate that microcantilevers modified with a chemically responsive coating produce large (micrometer-scale) bending responses in the presence of vapor-phase TNT and its analogs, 1-mononitrotoluene (1-MNT) and 2,4-dinitrotoluene (2,4-DNT). Efficient delivery of low-vapor-pressure nitroaromatic analytes was achieved by heating the analyte delivery system and encasing the detector in a heatable flow cell. The magnitude of responses to TNT vapor increased and the response kinetics was dramatically accelerated as the detector temperature was raised from 22 °C to 40 °C. The noise-limited TNT detection threshold was estimated to be 520 ppt_v.

Keywords: Microcantilever, Explosives, Detector.

1. INTRODUCTION

1.1. Background

Recent events have raised the concern of facing deadly chemical and biological toxins in common urban environments as a result of chemical and biological warfare proliferation, terrorist activities, or accidental contamination. This indicates an increasing need for rapid and reliable detection of hazardous or regulated substances, including explosives. It has been widely discussed[1] that detection of nitroaromatic explosive compounds is a highly significant task in forensics, antiterrorist activities, and global de-mining projects. In particular, the ability to detect trace levels of trinitrotoluene (TNT) in air and soil could become a key measure in reducing continued fatalities from land mines among civilians as well as tracking and locating explosive materials.

In recent years, several alternative detection strategies have been pursued to develop warning systems that could provide sensitive and selective identification of explosive substances.[1, 2] Previously described approaches to sensitive detection of nitroaromatic explosive substances are based on immunossays,[3–5] fluorescence measurements,[6–9] Raman spectroscopy,[10, 11] electrochemistry,[12] ion mobility spectroscopy,[13] nuclear quadrupole resonance,[14–16] and IR spectroscopy.[17] Although each of these methods has inherent advantages and disadvantages, their common feature is a high degree of complexity that adversely affects their compatibility with miniature mass-deployable devices.

The main challenge of continuous, real-time detection of nitroaromatic explosive compounds is related to their extremely low vapor pressures and, respectively, concentrations in air at ambient temperatures. For instance, the saturated vapor pressure of TNT at 25 °C is only 7.7×10^{-4} Pa[2], which corresponds to approximately 70 μg m^{-3} or 13 ppb_v. It has been discussed in the literature that typical concentrations of TNT in the vicinity of buried land mines or packaged explosive devices can be one to two orders of magnitude less than the concentration of saturated TNT vapor.[1, 18] Obviously, elevated ambient temperatures lead to higher concentrations of TNT vapor and simplify the detection of explosives. By contrast, real-time (without preconcentration) detection of TNT vapor in cold environ-

*Corresponding author; E-mail: datskospg@ornl.gov

ments can be extremely difficult. It is reasonable to assume that there is a critical ambient temperature below which any method of detecting TNT in air becomes inefficient. On the other hand, sampling techniques may involve preheating the area or objects to be inspected.

Because it is very difficult, if not impossible, to address the challenges of vapor-phase TNT detection with the majority of the previously explored methods, attention has recently been drawn to highly sensitive gravimetric transducers modified with molecular recognition coatings selective for respective nitroaromatic molecules. Some of the most successful embodiments of this concept include surface acoustic wave (SAW) devices coated with fluoro-alcohol and cyclodextrin-modified polymers.[18, 19] A further advantage can be created by replacing SAW devices with microcantilever transducers[20] or using microcantilevers as a calorimetric spectrometer.[21] Sensors based on microcantilever transducers[22] feature superior mass sensitivity, smaller sizes, lower cost, and excellent compatibility with large multisensor arrays.

Our recent studies have focused on the design of microcantilever sensors in which weak chemical or biochemical stimuli can be converted into mechanical responses with very high efficiency. As we discussed previously, efforts in this direction have multiple objectives.[23–27] In particular, by developing nanomechanical transducers with a high intrinsic gain, we address issues of improved sensitivity and signal-to-noise ratios.[23–27] Furthermore, large (micrometer-scale) mechanical responses produced by such high-gain microcantilever sensors can be read out with very simple means. More importantly, highly efficient chemimechanical transducers can be used as platforms for innovative sensors powered exclusively by the energy of analyte–device interactions.

One of our approaches to enhanced chemimechanical transduction is based on the use of microcantilevers with nanostructured surfaces or coatings. Several "top-down" and "bottom-up" strategies were explored in recent work to create appropriate phases with nanoscale 3-D features, such as crevices, gaps, and pores.[23–27] In many instances, the use of nanostructured coatings resulted in two-order-of-magnitude enhancements in analyte-induced microcantilever deflections.[23–27]

In the present study, we demonstrate that a standard atomic force microscope (AFM) microcantilever modified with a relatively thick (~0.5 μm) nanoporous organic coating can function as a detector of TNT vapors with a high intrinsic gain. To prepare a chemically responsive nanoporous layer, we used a compound of the calixarene family,[28, 29] namely *tert*-butylcalix[6]arene (TBC6A). Thin (0.1 to 1 μm) uniform films of TBC6A can be readily formed on solid substrates by physical vapor deposition (PVD) in a vacuum.[21, 30] TBC6A belongs to the class of macrocyclic oligomers commonly referred to as cavitand hosts because their molecules resemble baskets or caps with cavities of molecular dimensions inside.[28] Each TBC6A molecule contains six phenol units and measure approximately 1.5 nm in diameter with a height of 0.4 nm.[28, 29] We anticipated that chemical affinity of TBC6A with respect to TNT may originate from (i) reciprocal hydrogen donating–accepting interactions between -OH (host) and -NO_2 (guest) groups, respectively; (ii) π-stacking between host and guest aromatic moieties; and (iii) a basket-like molecular shape of the macrocycle.[31–33] We observed micrometer-scale deflections of the microcantilever with a TBC6A coating in response to vapors of TNT and its analogs, 1-mononitrotoluene (1-MNT), 2,4-dinitrotoluene (2,4-DNT), and TNT vapors.

1.2. Mechanisms of Cantilever Responses

To design microcantilever sensors with optimized parameters, two distinctive models[34] of cantilever responses need to be evaluated. The first model (Fig. 1a) is most adequate when interactions between a microcantilever and its environment are purely surface phenomena. It was shown that microcantilevers are suitable for real-time measurements of surface stress changes in the low mN m^{-1} range (Ref. 35) and, therefore, capable of converting changes in the Gibbs free energy due to binding site–analyte interactions into readily measurable mechanical responses. A microcantilever intended for chemical sensing can be modified so that one of its sides is relatively passive while the other exhibits high affinity for the targeted analyte. Consequently, changes in differential surface stress can be governed primarily by changes in Gibbs free energy associated with adsorption (surface interaction) processes on the active side. Chemisorption of straight-chain thiol molecules on a gold-coated silicon nitride cantilever (see Fig. 1a) is an example of this situation. Adsorbate-induced deflections can

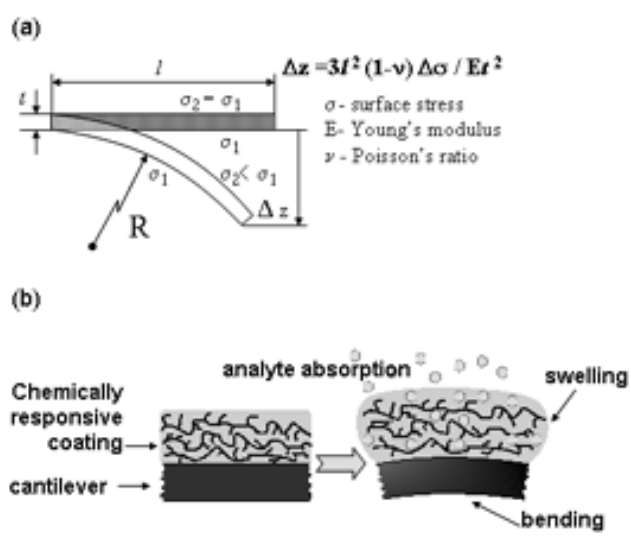

Figure 1. Mechanisms of cantilever responses: (a) Deformations induced by true surface interaction (adsorption) on smooth surfaces modified with a thin responsive coating impermeable to analytes. (b) Absorption-induced deformations in the case of thicker, analyte-permeable coatings.

be described analytically with a modification of the equation proposed by Stoney.[36] Stoney's equation is readily applicable when adsorbate-induced stresses are generated on ideal, analyte-impermeable, smooth surfaces.

The second model of analyte-induced stresses is applicable when a microcantilever is modified with thicker, analyte-permeable coatings (Fig. 1b). In this case, interactions of the analyte molecules with the bulk of the responsive phase should be taken into account, and a predominant mechanism of cantilever deflection can be described as analyte-induced swelling of the coating (Fig. 1b). In the case of nanoporous coatings, such swelling processes can be quantified by approaches similar to those developed in colloidal and polymer science, that is, by evaluating molecular forces acting in the coating and between the coating and the analyte species. In general, dispersion, electrostatic, steric, osmotic, and solvation forces acting within the coating can be expected to change upon analyte binding.

Analysis of the above models indicates that there are several important advantages of responsive coatings with nanoporous structure and thicknesses larger than 10 nm. The main advantages of thicker nanoporous coatings are (i) very high surface density of binding sites (since each cavitand molecule represents at least one binding site) and (ii) accessibility of the coating bulk to analyte molecules. The resulting swelling caused by molecular *absorption*,[34] rather than *adsorption*, provides a very efficient transduction of chemical interactions into mechanical stress. Cantilever deformations associated with absorption-induced swelling of responsive coatings can be quantified in analogy to temperature-induced deformations in bimaterial cantilevers.[37, 38] It is worth noting that the magnitude of cantilever bending responses predicted by this model scale up nearly proportionally to the responsive coating thickness. Such dependencies were confirmed in our previous experiments for 10–500-nm-thick coatings.[23, 27] This trend, however, may start to break down when the coating exceeds a certain thickness.[23] The critical thickness is primarily defined by two factors: (i) contribution of the coating stiffness to the total stiffness of the cantilever and (ii) loss of the coating integrity as analyte-induced stresses are built up. It is also worth noting that the deposition of coatings thicker than 1 μm often results in an unacceptably strong deformation of the microcantilever. Furthermore, diffusion of analyte into and out of thicker coatings may become an additional factor responsible for slower response and recovery kinetics.

2. EXPERIMENTAL DETAILS

The nitroaromatic compounds 1-MNT, and 2,4-DNT (98% purity) were obtained from Aldrich. TNT was obtained from Chem Services, Inc., with a stated purity of 98%. TBC6A (96% purity) was obtained from Acros Organics. Commercially available gold-coated silicon nitride AFM cantilevers (Park Scientific, Inc.) were used in the present studies. The cantilevers were triangular in shape, with a tip-to-base length of 320 μm. The thicknesses of the silicon nitride cantilever and the gold coating were, respectively, 500 nm and 40 nm. Subsequently, the microcantilevers were coated with TBC6A in vacuum, by PVD procedures similar to those described previously.[25, 27, 30] The resulting devices had a trilayer structure, which is shown schematically in Figure 2a. We selected a thickness of 500 nm for the TBC6A coatings, taking into account results of our previous[21, 25, 27] as well as ongoing studies on microcantilever detectors coated with TBC6A and similar responsive phases.

The microcantilever deflection measurements were made with the optical beam-deflection technique. Our apparatus, described previously in more detail,[27] included a 5-mW diode laser (Coherent Laser Corp., Auburn, CA) operating at 635 nm, a focusing system, and a position-sensitive photodetector. The amplified output signal of the photodetector

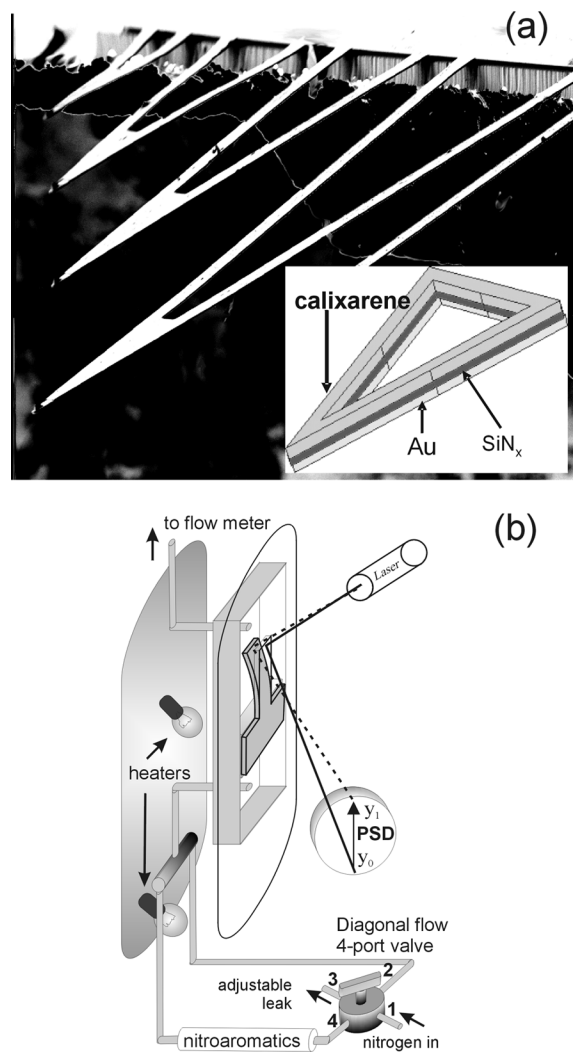

Figure 2. (a) Electron scanning micrograph of microcantilevers used and schematics of their layered structure after modification with a TBC6A coating. (b) Schematics of vapor generator and analyte delivery systems used in the present studies.

was displayed and recorded with a multichannel digital recorder (Stanford Research Systems, Sunnyvale, CA). The conversion factor for converting the measured output voltage to microcantilever tip deflection was determined by displacing the detector with a micrometer and measuring the corresponding change in output voltage. With knowledge of the optical geometry it is possible to convert the output voltage into cantilever tip deflections. The cantilever was mounted inside a 1.5×10^{-7} m^3 Teflon flow cell that was imaged with a CCD camera equipped with a microscope zoom lens. Nitrogen was used as the carrier gas. The flow of nitrogen gas was delivered to the flow cell via stainless-steel tubing connected to a four-port diagonal flow valve, allowing for switching between the pure nitrogen and a nitrogen equilibrated with analyte vapor at room temperature (Fig. 2b). The two flow pathways were combined by means of a stainless-steel T-connector. The flow rate measured at the flow cell outlet was adjusted to 1.6×10^{-7} m^3 s^{-1}. Both the flow cell and the stainless-steel part of the gas delivery system were placed inside a thermally insulated enclosure with two heaters, allowing for separate temperature control of the flow cell and the inlet tubing (see Fig. 2b). Miniature halogen lamps (20 watts) were used as heating sources that allowed us to change the temperature of the cell. Measurements of the temperature were made with a thermocouple thermometer. The entire apparatus was placed on a vibration isolation table located in a thermally controlled environment. Care was taken to maintain all parts of the apparatus outside the heated enclosure at room temperature.

Saturated vapor of 1-MNT was generated with a syringe pump with a 5 cm^3 syringe that was loaded with 0.1 cm^3 of 1-MNT and filled with nitrogen. The vapor from a syringe pump was mixed with pure nitrogen gas with the T-connector. To generate vapors of 2,4-DNT and TNT, a piece of precleaned glass tubing was loaded with a small amount of the solid analyte and inserted between one of the two inlets of the T-connector and the diagonal flow valve. The other line was directly connected to the diagonal flow valve as shown in Figure 2b.

Loading of the glass tube (10 cm long and 5-mm inside diameter) with an analyte was performed by distributing approximately 10^{-8} m^3 of 2,4-DNT or TNT solution in chloroform (10^3 g m^{-3}) on the inner walls of the tube and allowing the tube to dry for an hour in air at room temperature. The same procedure was used in "blank" experiments, except that pure chloroform instead of an analyte solution was spread.

3. RESULTS AND DISCUSSION

We investigated bending responses of microcantilevers coated with TBC6A, which served as a nanoporous, chemically responsive layer. The vapor pressure, P, of the nitroaromatic compounds used in our studies progressively decreases with increasing number of nitro group: $P_{1\text{-MNT}} > P_{2,4\text{-DNT}} > P_{\text{TNT}}$. Mononitrotoluenes have relatively high vapor pressures at room temperature[39] and can be used as explosive simulants.[18] We used 1-MNT in our preliminary experiment to verify the sensitivity of the prepared functionalized cantilevers to nitroaromatics. Cantilever deflections in response to 1-MNT vapor are shown Figure 3. The carrier gas was nitrogen, and the vapor dilution was achieved by mixing saturated 1-MNT vapors from a syringe pump into a stream of pure carrier gas (nitrogen). By adjusting the delivery rate of saturated 1-MNT vapors, we obtained dilution ratios of 1:1000 and 1:100. Based on the data presented in Figure 3, we estimated that the threshold sensitivity of the calixerene-coated cantilever to 1-MNT vapor corresponds to a dilution ratio of 1:1000.

As compared with 1-MNT, both 2,4-DNT and TNT have much lower vapor pressures at room temperature[40, 41] and tend to form solid condensates on exposed surfaces under ambient conditions. To avoid condensation of 2,4-DNT and TNT on the inner surfaces of the analyte delivery system and the flow cell, the flow cell was kept at elevated temperatures between 35 °C and 45 °C while the inlet tubing was kept approximately 25 °C higher than the flow cell that contained the microcantilever transducer (Fig. 2b). Inasmuch as the cantilever had a trimaterial structure (calixarene/SiN_x/Au; see Fig. 2a) and was expected to respond to temperature changes, we quantified the effect of temperature before experiments with 2,4-DNT and TNT. Figure 4 shows the response of the coated cantilever to temperature changes from 25 °C to 35 °C. As can be seen in Figure 4, the cantilever responded reversibly to a temperature cycle from the ambient (22 °C) to the operational temperature of 35 °C. Although the thermal time constant of the microcantilever was approximately 10 ms, the observed slow kinetics of the thermal responses was determined primarily by the thermal time constant of the whole system, which included the cell and the analyte delivery lines. Under steady-state conditions, the microcantilevers were found to bend about 4.65 μm in response to a 13 °C temperature

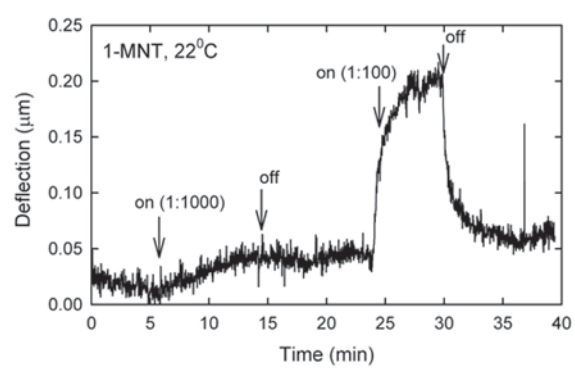

Figure 3. Responses of the TC6A-coated cantilever to dilute 1-MNT vapor in nitrogen. The vapor dilution was achieved by injecting saturated 1-MNT vapors into a stream of nitrogen carrier gas. The carrier gas flow rate was 10 ml/min (1.6×10^{-7} m^3 s^{-1}). By adjustment of the injection rate of saturated 1-MNT vapor (delivered by a syringe pump), a dilution ratio of 1:1000 to 1:100 was obtained. Threshold sensitivity corresponded to a dilution ratio of 1:1000.

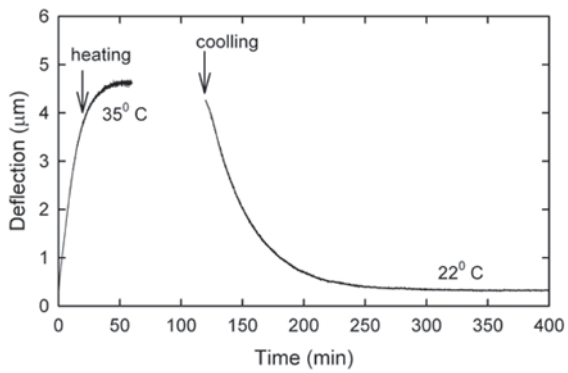

Figure 4. Responses of the TBC6A-coated cantilever to temperature changes. The cantilever is trimaterial (see Fig. 2) and responds to temperature changes. Elevated temperatures (above 35 °C) of the flow system are typically required for efficient delivery of 2,4-DNT or TNT. The tested microcantilever responded reversibly to a temperature cycle from 22 °C to 35 °C. Differential deflection measurements with a pair of appropriately designed cantilevers will ultimately compensate for the observed temperature effect.

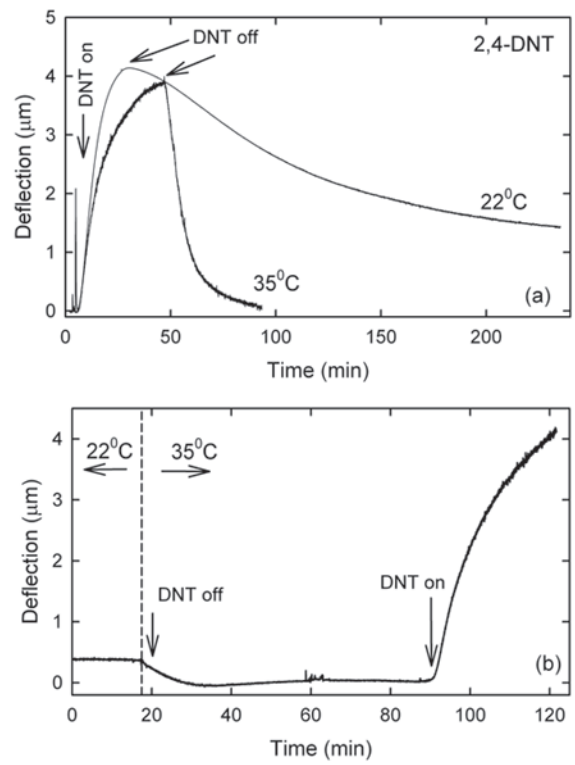

Figure 5. (a) Reversible responses and good sensitivity were observed at both room temperature (22 °C) and 35 °C. At 22 °C, the recovery kinetics was slow. The recovery accelerated significantly when the temperature of the flow cell and the analyte delivery system increased to 35 °C. (b) The recovery of the cantilever after exposure to 2,4-DNT takes more than 4 h at room temperature. The sensor exposed to 2,4-DNT and kept at room temperature can be rapidly regenerated by heating it to 35 °C.

change. However, the bending of the trilayer microcantilever due to increases in temperature was opposite in direction to the bending due to chemical response. Nonetheless, this notably high temperature sensitivity was kept in mind when cantilever responses to chemical analytes were interpreted. To compensate for any observed temperature effects, previously established approaches,[22] such as a sample–reference pair of appropriately designed cantilevers or cantilever arrays,[42, 43] can be used in future sensor designs.

Figure 5a shows the measured deflection of the TBC6A-coated cantilever in response to 2,4-DNT vapor as a function of time. The response was initiated by switching the inlet port of the flow cell from pure nitrogen to 2,4-DNT vapors generated in the glass tube that contained the analyte at room temperature (see Fig. 2b). Therefore, concentration of the 2,4-DNT delivered to the detector was defined by the vapor pressure of 2,4-DNT at 22 °C, that is, 1.65 mg m^{-3} or 200 ppb_v (Refs. 18, 40, 41). We observed reversible responses and good sensitivity for the detector temperatures of 22 °C and 35 °C. However, the recovery was slow at 22 °C (see Fig. 5a). Under a continuous flow of 2,4-DNT vapor through the flow cell, the cantilever approached a steady state in about 50 min at room temperature. The complete recovery of the system after exposure to 2,4-DNT required more than 4 h at room temperature. As can be seen from Figure 5a, the kinetics accelerated significantly when the temperature of the detector and the flow cell was raised to 35 °C.

The data shown in Figure 5a were used to estimate time constants for both "on" and "off" rates by fitting the respective parts of the data to an exponential transient function. We found that, at room temperature, the "on" and "off" rates are characterized by time constants of, respectively, 8 min and 160 min. When the detector temperature was raised to 35 °C, the estimated "on" and "off" time constants were found to be, respectively, 13 min and 9 min. An important question arises as to whether these time constants can be attributed to intrinsic processes in the microcantilever detector, such as adsorption/desorption of the analyte, or whether transport of the analyte through the flow system is responsible for the observed kinetics. In principle, a somewhat longer response time at 35 °C can be explained by a shift in adsorption/desorption equilibrium toward desorption. The decreased recovery time at elevated temperatures is also consistent with the model of thermally activated analyte desorption. At this point, however, we cannot exclude the possibility that desorption of 2,4-DNT from the inner surfaces of the flow system rather than from the detector itself could have made the predominant contribution into the observed slow "off" rates. It is reasonable to assume that at least two distinct mechanisms are responsible for the faster recovery observed at higher temperatures: (i) faster transfer of analyte from the heated flow system and (ii) accelerated, thermally activated desorption of the analyte molecules from the responsive coating.

Figure 5b shows the behavior of the cantilever exposed to 2,4-DNT when the temperature was raised from 22 °C to 35 °C during the recovery phase. In this case, the re-

sponse induced by the temperature change is a combination of the direct temperature effect on the cantilever bending and temperature-induced desorption of 2,4-DNT from the microcantilever surface. As it follows from the magnitude and the direction of the bending, the desorption effect is comparable to and slightly overcomes the thermally induced ("trimaterial") bending. The response observed upon subsequent exposure of the cantilever to 2,4-DNT vapor (see the last region of the response curve in Fig. 5b) confirms that the sensor was indeed regenerated while being heated from 22 °C to 35 °C; the two responses to the same concentration of 2,4-DNT shown in Figure 5 are of comparable magnitudes. Therefore, a possible sensor operation may consist of "sniffing" the analyte at room temperature and regenerating the sensor at 35 °C.

Figure 6 shows microcantilever deflections measured in response to TNT vapor. As in the case of 2,4-DNT, the concentration of TNT delivered to the detector was defined by its vapor pressure at 22 °C, that is, 13 ppb_v (Refs. 18, 40, and 41). The sensor exhibited very high responsivity to TNT, but both the response and the recovery were very slow. In fact, the sensor was not allowed enough time to reach a steady state during this set of experiments (Fig. 6a). The response and recovery time constants estimated from the kinetics observed at 30 °C are 140 min and 45 min, respectively. These observations are consistent with the previously documented fact that efficient delivery of TNT vapors to detectors with a flow system cannot be efficient unless the temperature of both the detector and the flow system is well above room temperature, typically 35 °C to 60 °C.[18] The difficulty of TNT vapor delivery is related to the extremely low vapor pressure of TNT at room temperature; TNT vapor tends to condense on all of the surfaces it comes in contact with. Subsequently, we verified that the observed responses were indeed due to the presence of TNT vapor and not to any possible artifacts related to the operation of our experimental system (see Fig. 6b).

Condensation of TNT vapors can be progressively reduced as the temperature approaches the melting point of TNT (80.9 °C). In our experiment, the difficulty of vapor-phase TNT delivery was largely eliminated by increasing the temperature of the flow system and the flow cell from 35 °C to 40 °C. When the temperature was increased to 40 °C, dramatically accelerated responses to TNT and moderately accelerated recovery of the sensor were observed (Fig. 7). Therefore, this small temperature increase was critical to providing much more efficient delivery of TNT molecules to the microcantilever sensor and to facilitating their interaction with the cavitand coating. The "on" and "off" rates observed for TNT at 40 °C corresponded to the time constants of 4 min and 32 min, respectively. The kinetic data obtained for the detector temperatures 35 °C and 40 °C indicate that the sensor response and recovery times rather than its sensitivity critically depend on the temperature. Although the response kinetics observed at 40 °C was

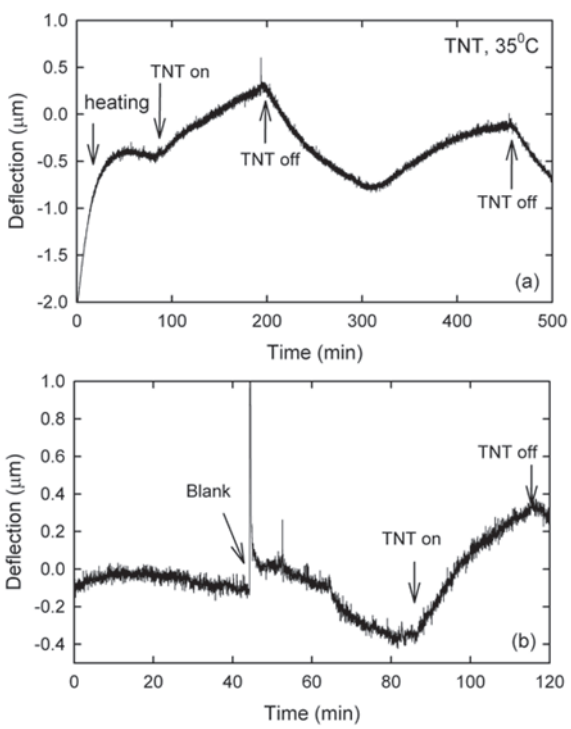

Figure 6. (a) The sensor exhibited good responsivity to TNT, but the response kinetics was slow and the sensor did not reach a steady state during this set of experiments. (b) The data shown demonstrate that the observed responses were due to the presence of TNT vapor and not to any possible artifacts related to the operation of the analyte delivery system.

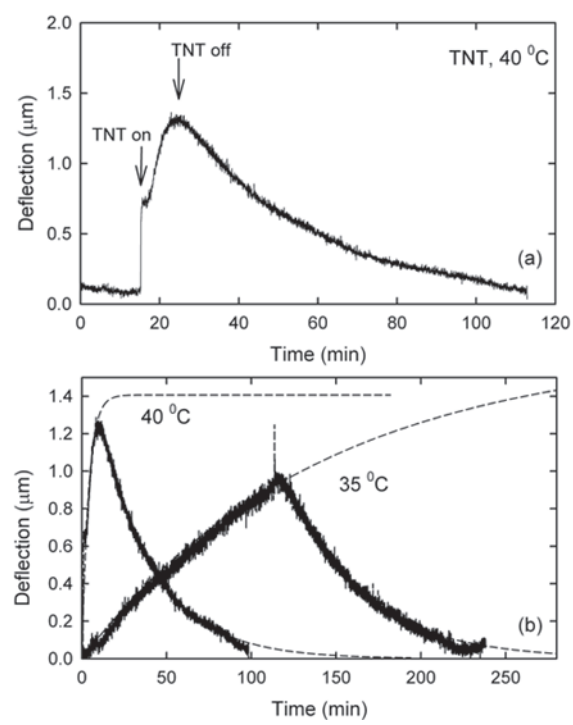

Figure 7. (a) At 40 °C, significantly accelerated responses to TNT and recovery of the sensor were observed. (b) Determining "on" and "off" time constants by fitting the kinetics measured for TNT at 35 °C and 40 °C to exponential transient functions.

sufficiently fast from a practical point of view, the much slower "off" rate during the recovery process indicates that further optimization of the thermal regime might be needed.

Because of the technical challenge of controllable dilution of TNT vapor, we have not studied responses to TNT in the range of concentrations below saturation. However, our data obtained previously[21, 25–27] for a variety of other analytes indicate that, as a rule, magnitudes of responses of microcantilever sensors are nearly proportional to the analyte concentrations. Although calibration curves deviated somewhat from the linear at the high end of the concentration range, dynamic ranges of up to two orders of magnitude were commonly observed.[21, 27] Therefore, the dynamic range and the limit of detection of the proposed sensor can be based on the linear extrapolation of the data obtained for saturated vapor. By assuming the noise level to be 10 nm, we obtained a LOD of 520 ppt for detection of TNT with a signal-to-noise ratio of 3:1.

The results of our continued work with TBC6A coatings indicate the operational life of the proposed sensors to be on the order of months. Taking into account the low cost of microcantilever sensors, this level of durability can even be somewhat redundant. In general, however, cycling stresses may result in sensor degradation. Our recent studies[25–27] showed that microcantilevers with micro- or nanostructured surfaces are much less prone to the possible degradation or stress-slip conditions.

4. CONCLUSIONS

Bending responses of a microcantilever sensor to a series of vapor-phase nitroaromatic compounds were quantified in the range of temperatures of 22 °C to 40 °C. Vapor-phase TNT and 2,4-DNT saturated at room temperature induced reproducible and reversible deflections of a microcantilever transducer with magnitudes of up to 3 μm. These results demonstrate the feasibility of a cantilever-based TNT sensor with a very high intrinsic gain. Although the responsivity of the proposed sensor system was remarkably high, the detector and the flow system had to be heated to 40 °C to reach practically useful response and recovery times. Assuming the noise level to be a conservative 10-nm deflection, we estimated that the LOD of the proposed microcantilever sensor for TNT to be 520 ppt_v. Deflection noise levels of 1 nm are possible, which will lower the estimated LOD by an order of magnitude.

Taking into account our present findings, we envision engineering a functional prototype of the cantilever-based TNT detector that will involve further refinements, such as optimization of the temperature regime and use of a differential pair of cantilever transducers or multiple cantilever transducers arranged in an array. Although the reported experiments employed precision optical components assembled on vibration isolation mounts, we are currently working toward a portable bench-top optical readout system that would provide similar performance. The feasibility of such a readout system is clearly indicated by the feasibility of precision optical CD readout widely used in CD players. Furthermore, because microcantilever detectors have masses on the order of a few 10^{-9} g, ramping their temperatures from 22 °C to above 40 °C can be achieved within a subsecond time frame. Therefore, it would be possible to implement a dynamic temperature regime (flash desorption) to rapidly regenerate sensors after exposure to TNT. In summary, the results reported here, together with the previously established advantages of microcantilever-based gas detectors, clearly indicate a viable technological approach to mass-produced detectors of explosive materials.

Acknowledgments: We acknowledge support from the EMSP program of the Department of Energy. This work was partially supported by the Laboratory Director's Research and Development Program of Oak Ridge National Laboratory. Oak Ridge National Laboratory is operated for the U.S. Department of Energy by UT-Battelle under contract DE-AC05-96OR22464.

References and Notes

1. J. I. Steinfeld and J. Wormhoudt, *Annu. Rev. Phys. Chem.* 49, 203 **(1998)**.
2. J. Yinon, *Trends Anal. Chem.* 21, 292 **(2002)**.
3. J. C. Bart, L. L. Judd, and A. W. Kusterbeck, *Sens. Actuators, B* 39, 411 **(1997)**.
4. S. Y. Rabbany, W. J. Lane, W. A. Marganski, A. W. Kusterbeck, and F. S. Ligler, *J. Immunol. Methods* 246, 69 **(2000)**.
5. J. P. Whelan, A. W. Kusterbeck, G. A. Wemhoff, R. Bredehorst, and F. S. Ligler, *Anal. Chem.* 65, 3561 **(1993)**.
6. K. J. Albert and D. R. Walt, *Anal. Chem.* 72, 1947 **(2000)**.
7. K. J. Albert, M. L. Myrick, S. B. Brown, D. L. James, F. P. Milanovich, and D. R. Walt, *Environ. Sci. Technol.* 35, 3193 **(2001)**.
8. T. Arusi-Parpar, D. Heflinger, and R. Lavi, *Appl. Opt.* 40, 6677 **(2001)**.
9. C. J. Cumming, C. Aker, M. Fisher, M. Fox, M. J. la Grone, D. Reust, M. G. Rockley, T. M. Swager, E. Towers, and V. Williams, *IEEE Trans. Geosci. Remote* 39, 1119 **(2001)**.
10. N. Gupta and R. Dahmani, *Spectrochim. Acta A* 56, 1453 **(2000)**.
11. J. M. Sylvia, J. A. Janni, J. D. Klein, and K. M. Spencer, *Anal. Chem.* 72, 5834 **(2000)**.
12. W. J. Buttner, M. Findlay, W. Vickers, W. M. Davis, E. R. Cespedes, S. Cooper, and J. W. Adams, *Anal. Chim. Acta* 341, 63 **(1997)**.
13. R. G. Ewing, D. A. Atkinson, G. A. Eiceman, and G. J. Ewing, *Talanta* 54, 515 **(2001)**.
14. A. N. Garroway, M. L. Buess, J. B. Miller, B. H. Suits, A. D. Hibbs, G. A. Barrall, R. Matthews, and L. J. Burnett, *IEEE Trans. Geosci. Remote* 39, 1108 **(2001)**.
15. K. P. Kirkbride, G. Klass, and P. E. Pigou, *J. Forensic Sci.* 43, 76 **(1998)**.
16. T. N. Rudakov, V. T. Mikhaltsevich, and O. P. Selchikhin, *J. Phys. D Appl. Phys.* 30, 1377 **(1997)**.
17. M. W. Todd, R. A. Provencal, T. G. Owano, B. A. Paldus, A. Kachanov, K. L. Vodopyanov, M. Hunter, S. L. Coy, J. I. Steinfeld, and J. T. Arnold, *Appl. Phys. B* 75, 367 **(2002)**.
18. X. G. Yang, X. X. Du, J. X. Shi, and B. Swanson, *Talanta* 54, 439 **(2001)**.
19. E. J. Houser, T. E. Mlsna, V. K. Nguyen, R. Chung, R. L. Mowery, and R. A. McGill, *Talanta* 54, 469 **(2001)**.
20. L. A. Pinnaduwage, V. Boiadjiev, J. E. Hawk, and T. Thundat, *Appl. Phys. Lett.* 83, 1471 **(2003)**.

21. P. G. Datskos, S. Rajic, M. J. Sepaniak, N. Lavrik, C. A. Tipple, L. R. Senesac, and I. Datskou, *J. Vac. Sci. Technol., B* 19, 1173 (**2001**).
22. M. Sepaniak, P. Datskos, N. Lavrik, and C. Tipple, *Anal. Chem*. 74, 568A (**2002**).
23. N. V. Lavrik, C. A. Tipple, M. J. Sepaniak, and P. G. Datskos, *Biomed. Microdevices* 3, 35 (**2001**).
24. N. V. Lavrik, C. A. Tipple, M. J. Sepaniak, and P. G. Datskos, *Proc. SPIE* 4560, 152 (**2001**).
25. J. J. Headrick, M. J. Sepaniak, N. V. Lavrik, and P. G. Datskos, *Ultramicroscopy* 97, 417 (**2003**).
26. N. V. Lavrik, C. A. Tipple, M. J. Sepaniak, and P. G. Datskos, *Chem. Phys. Lett*. 336, 371 (**2001**).
27. C. A. Tipple, N. V. Lavrik, M. Culha, J. Headrick, P. Datskos, and M. J. Sepaniak, *Anal. Chem*. 74, 3118 (**2002**).
28. C. D. Gutsche, *Acc. Chem. Res*. 16, 161 (**1983**).
29. E. Vandienst, W. I. I. Bakker, J. F. J. Engbersen, W. Verboom, and D. N. Reinhoudt, *Pure Appl. Chem*. 65, 387 (**1993**).
30. A. Dominik, H. J. Roth, and W. Gopel, *Supramol. Sci*. 1, 11 (**1994**).
31. D. Diamond and M. A. McKervey, *Chem. Soc. Rev*. 25, 15 (**1996**).
32. K. D. Schierbaum, A. Gerlach, W. Gopel, W. M. Muller, F. Vogtle, A. Dominik, and H. J. Roth, *Fresenius' J. Anal. Chem*. 349, 372 (**1994**).
33. A. Arduini, F. F. Nachtigall, A. Pochini, A. Secchi, and F. Ugozzoli, *Supramol. Chem*. 12, 273 (**2000**).
34. Z. Y. Hu, T. Thundat, and R. J. Warmack, *J. Appl. Phys*. 90, 427 (**2001**).
35. H. J. Butt, *J. Colloid. Interface Sci*. 180, 251 (**1996**).
36. G. G. Stoney, *Proc. R. Soc. London, Ser. A* 82, 172 (**1909**).
37. P. J. Shaver, *Rev. Sci. Instrum*. 40, 901 (**1969**).
38. S. P. Timoshenko, *J. Opt. Soc. Am*. 11, 233 (**1925**).
39. D. Ambrose and H. A. Gundry, *J. Chem. Thermodyn*. 12, 559 (**1980**).
40. L. Rittfeldt, *Anal. Chem*. 73, 2405 (**2001**).
41. A. Burcat, *J. Phys. Chem. Ref. Data* 28, 63 (**1999**).
42. H. P. Lang, R. Berger, F. Battiston, J. P. Ramseyer, E. Meyer, C. Andreoli, J. Brugger, P. Vettiger, M. Despont, T. Mezzacasa, L. Scandella, H. J. Guntherodt, C. Gerber, and J. K. Gimzewski, *Appl. Phys. A* 66, S61 (**1998**).
43. H. P. Lang, M. K. Baller, R. Berger, C. Gerber, J. K. Gimzewski, F. M. Battiston, P. Fornaro, J. P. Ramseyer, E. Meyer, and H. J. Guntherodt, *Anal. Chim. Acta* 393, 59 (**1999**).